

Solvent effects on the UV-visible absorption spectrum of benzophenone in water: A combined Monte Carlo quantum mechanics study including solute polarization

Herbert C. Georg,^{a)} Kaline Coutinho, and Sylvio Canuto

Instituto de Física, Universidade de São Paulo, CP 66318, São Paulo, Sao Paulo 05315-970, Brazil

(Received 24 October 2006; accepted 1 December 2006; published online 18 January 2007)

The entire ultraviolet-visible absorption spectrum of benzophenone in water is studied and compared with the same spectrum in gas phase. Five transitions are considered, and the corresponding solvatochromic shifts are obtained and compared to experiment. Using a sequential procedure of Monte Carlo simulations and quantum mechanical calculations, liquid configurations were generated and an averaged spectrum of the solution was calculated. The solute polarization was included by an iterative procedure where the atomic charges of the solute were obtained as an average with the solvent distribution. The calculated average dipole moment of benzophenone in water, with MP2/6-31++G(*d,p*), converges to the value of 5.84 ± 0.05 D, 88% larger than the gas-phase value of 3.11 D. Using 100 statistically uncorrelated configurations and solvation shells with 235 explicit water molecules selected by a minimum-distance distribution of solvent shells, instead of the usual radial distribution, the excitation energies were obtained from solute-solvent all-valence-electron INDO/CIS calculations. The shift of the weak $n-\pi^*$ transition is obtained as 2045 ± 40 cm^{-1} and the strong and broad $\pi-\pi^*$ shift as -1790 ± 30 cm^{-1} . These results are in good agreement with the experimental values of 2200 and -1600 cm^{-1} , respectively. Standard procedure used by common force fields to generate atomic charges to describe the electrostatic moments of the solute, with HF/6-31G(*d*), gives a dipole moment of 3.64 D. Using these standard charges in the simulation, the average shifts are calculated as 1395 ± 35 and -1220 ± 25 cm^{-1} , both about 600 cm^{-1} smaller in magnitude than those obtained with the average converged fully polarized solute. The influence of the solute polarization in the solute-solvent interaction and, in particular, in solute-solvent hydrogen bonds is analyzed. © 2007 American Institute of Physics.

[DOI: 10.1063/1.2426346]

I. INTRODUCTION

The study of the solvent effect on molecular properties is of immense scientific and technological interests. The solvent plays an important role in several processes, powering molecular properties, accelerating chemical reactions, and making feasible innumerable biological processes.¹ Onsager² and Kirkwood³ developed, in the early days of quantum mechanics, a model in which the solvent is treated as a continuum dielectric. These ideas were developed further to the concept of a self-consistent reaction field,⁴ where the dielectric is polarized by the charge distribution of the solute, which is in turn polarized by the field of the induced charges of the dielectric.

One drawback of the continuum models is that the specific interactions between the solute and the solvent need special considerations that are not always justified. An alternative approach where the solvent is treated explicitly has been developed.⁵ This approach recognizes the need for a statistical treatment of the liquid, and for a proper description, a large number of molecules must be included in the calculations. Since it is not feasible to perform fully quantum

mechanical simulations in such larger systems, the hybrid quantum mechanics/molecular mechanics (QM/MM) approach—where the region of interest is treated with quantum mechanics while the rest of the system is treated with empirical force fields—arises naturally.

A variant of the QM/MM method has been developed.^{6,7} In this method, the simulation of the liquid is performed in the MM level and, subsequently, QM calculations are performed with statistically uncorrelated configurations extracted from the simulation. This approach, called sequential QM/MM (S-QM/MM), has the advantage that all the statistical information is known before the QM calculations are performed, then permitting the selection of the statistically relevant configurations and the achievement of converged averages with relatively few QM calculations.

The intermolecular interaction potential plays a fundamental role in MM simulations and is also very important for adequate treatment of the solvent effects in QM/MM methodologies.⁸⁻¹¹ A great concern, in this aspect, is the polarization of the solute. Mostly, the empirical potentials used in liquid simulations include an *ad hoc* implicit polarization in the electrostatic parameters. The standard procedure is to use the HF/6-31G(*d*) calculation level¹² and it results typically in a 20% increase in the dipole moment of the molecules.¹³ In some cases this is probably enough to ac-

^{a)}Author to whom correspondence should be addressed. Fax: +55.11.3091-6831. Electronic mail: hcgeorg@if.usp.br

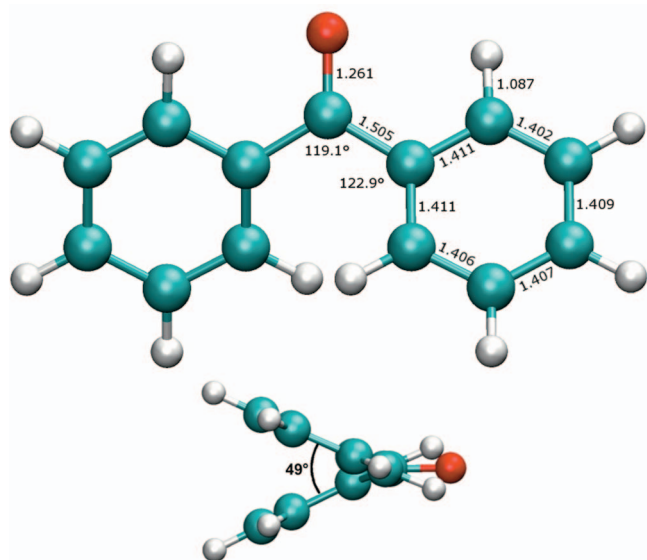


FIG. 1. (Color) Illustration of benzophenone in two perspectives and geometric parameters.

count for the electronic polarization, but in other cases the actual polarization can achieve higher values and a more thorough consideration of the polarization is needed. In fact, a more accurate description of the molecular polarization in liquid phase, and consequently of the intermolecular potential, is always desirable.

Some important theoretical studies have been done on the electronic polarization of a reference molecule in a liquid environment.^{8–17} The dipole moment of a single molecule embedded in a liquid environment is not easy to be evaluated experimentally. Indirect results can be inferred by integrating infrared intensities,¹⁸ for example, but only scarce estimates are available. Therefore a reliable theoretical procedure to predict dipole moments in liquid phase is of great interest, and computer simulation is a natural way to carry out this type of calculation.

A systematic procedure for obtaining the electronic polarization of a reference molecule in liquid environment, based on the iterative use of the S-QM/MM method, has been briefly described in a previous article.¹⁹ In that work we applied the method to calculate the dipole moment of acetone in liquid water and obtained a converged average value of 4.80 ± 0.30 D (the uncertainty being the standard deviation), corresponding to a large increase of 60% from the gas-phase value. To probe that, we used the converged average atomic charges in an extra simulation of the acetone dilute solution. Then, using the S-QM/MM methodology, we obtained a converged average shift of 1650 cm^{-1} for the $n-\pi^*$ transition, in very good agreement with the experimental shift^{20–22} that lies between 1500 and 1700 cm^{-1} . This represents an improvement to the shift of 1296 cm^{-1} that is obtained using the standard *ad hoc* procedure to generate the atomic charges for acetone.²³ A more significant effect could be expected for a more polarizable molecule such as benzophenone.

In the present work we study the solvatochromic shift on the UV-visible absorption spectrum of benzophenone (see Fig. 1) in water. This is an interesting system showing di-

verse solvatochromic effects. The experimental absorption spectrum of benzophenone is characterized by two broad bands.²⁴ The first is a weak $n-\pi^*$ band in the region of $320\text{--}370 \text{ nm}$ and the second is a strong band in the region of $240\text{--}300 \text{ nm}$ that corresponds to several $\pi-\pi^*$ transitions. These bands show large and distinct solvent dependence. The $n-\pi^*$ transition, for instance, suffers a strong blueshift of approximately 2200 cm^{-1} from *n*-hexane to water, while the $\pi-\pi^*$ band maximum suffers a redshift of around 1600 cm^{-1} . The UV-vis absorption spectrum of benzophenone is also important in many other contexts and in special it has been used as a probe in characterizing supercritical properties of water.²⁵

Describing the solvatochromic shift of such spectrum is a theoretical challenge, since different solvation processes must be treated to describe both shifts simultaneously. An early study²⁶ obtained qualitatively correct shifts for the UV-vis spectrum of benzophenone in water combining a classical Monte Carlo simulation for generating the liquid structures and the INDO/CIS method²⁷ to obtain the spectrum. A blueshift of 1170 cm^{-1} in the $n-\pi^*$ transition and a redshift of 1332 cm^{-1} in the $\pi-\pi^*$ transition were found considering a hydration shell of 20 water molecules.

In the present article we analyze the entire UV-vis absorption spectrum of benzophenone (up to $45\,000 \text{ cm}^{-1}$) in water considering extended solvation shells and the solute polarization. As we shall see, an accurate description of the benzophenone spectrum in water is obtained after considering a systematic and converged procedure to describe the solute polarization and after reconsideration of the definition of the solvation shell that gives the distribution of solvent molecules around the solute.

II. CALCULATION METHODOLOGY

A. Solute polarization

We have recently developed a procedure to describe the electronic polarization of a molecule in solution.¹⁹ In this procedure we iteratively apply the S-QM/MM methodology to calculate the dipole moment of the solute molecule in the presence of the solvent.

Using initial atomic charges for the solute [derived via *ab initio* calculation of the electrostatic potential (EP) of the molecule followed by a charges from electrostatic potentials using a grid (CHELPG) fit²⁸] corresponding to the gas-phase electronic distribution, the configurations of the liquid are generated by Monte Carlo classical simulation. Next, statistically uncorrelated configurations of the liquid are selected to calculate the average dipole moment of the solute in the presence of the solvent (represented by fixed partial charges corresponding to the employed water model). Hence, at this stage, the solute will respond to the field produced by the solvent giving rise to new induced multipoles. Along with the dipole moment, the EP generated by the new electronic distribution of the solute is calculated and the atomic charges are fitted for each configuration.

The average atomic charges are then used to perform another simulation, in which the solvent molecules will be permitted to rearrange in a different structure, and so on.

This is carried out until the average dipole moment converges, giving the in-solution value of the dipole moment of the solute molecule. When this convergence is achieved, the interaction energy gained with the rearrangement of the solvent around the solute is comparable to the thermal energy. At this point, the solute will be in electrostatic equilibrium with the environment. In this work, all these calculations are performed at the second-order MP2 level. In this application, we are mainly concerned about the polarization of the solute and we assume a fixed polarization of the solvent.

Similar procedures^{9,10,14} have been developed to account for the electronic polarization. In particular, Martin *et al.*^{14,29} have developed a procedure based on the averaged value of the solvent electrostatic potential (ASEP). In their approach, the potential provided by the solvent is averaged and the resulting mean field is considered as a perturbation to the solute molecular Hamiltonian, through which new atomic charges are calculated. In our present method, in each iteration step, the dipole moment and atomic charges are given by a converged average over several (in the present case, 100) uncorrelated configurations as prescribed by the S-QM/MM method.

It is important to stress that the convergence of the dipole moment in each step of the iteration process is assured because of the statistical analysis by which we are able to select statistically uncorrelated configurations from the simulation to perform the QM calculations.

Each simulation is made with calculated average atomic charges and consequently the charge fluctuation of the solute is not considered. Early theoretical works have considered this aspect^{30,31} and have shown that charge fluctuation of the solute may be significant for excited states but less important for the ground state.^{30,31} We thus expect this to have a small effect on the Franck-Condon transition from the ground state. As we use fixed charges in the solvent, the solute fluctuation will mainly alter the solvent structure. Hence we assume that the solvent structural reorganization is slow compared to the fluctuation of the solute dipole such that the net influence can be represented by the average polarized solute dipole moment.

B. Calculation details

The liquid configurations are generated by Monte Carlo (MC) Metropolis simulations in the *NPT* ensemble using standard procedures.^{6,7,32} The DICE program³³ was used to perform the MC simulations. The system is composed of 1 benzophenone molecule and 700 water molecules and is kept at room temperature (298 K) and pressure (1 atm). Periodic boundary conditions are used in a parallelogramic box with approximate dimensions of 31.8, 27.4, and 24.6 Å. This type of box accommodates the water molecules around the benzophenone solute better. Considering that the characteristic dimensions of benzophenone are 11.5, 7.0, and 4.0 Å, in the three directions there is a ~ 10 Å buffer of water between the molecule and the box walls.

The molecules interact by the Lennard-Jones (LJ) plus

Coulomb (LJC) potential. The LJ parameters are kept fixed during the iteration process, while the Coulomb part of the solute is adjusted to the actual ambient.

For the water molecules we employed the simple point charge model.³⁴ The geometry of benzophenone is that obtained before²⁶ to facilitate comparison and it is in good accord with the x ray-derived geometry.³⁵ The geometry is kept rigid during the whole process. The partial charges for benzophenone are obtained by fitting the electrostatic potential calculated with MP2/6-31++G(*d,p*) via CHELPG (Ref. 28) using the GAUSSIAN 98 program.³⁶ For each configuration the total charge in the solute is of course zero. Taking the average could slightly break this but we never found this problem within five decimal figures used here. The LJ parameters used for benzophenone are taken from the OPLS set.³⁷

After equilibration, the production simulations are carried out for 70×10^6 steps. The average density obtained in the first step is 0.997 ± 0.009 g/cm³, equivalent to the density of pure water and it increases slightly, up to 0.999 ± 0.010 g/cm³, in the last iteration step of the polarization procedure. During the production simulation, a preferential sampling scheme³⁸ is employed so that the probability of choosing a water molecule to translate and rotate is inversely proportional to the square distance between that water molecule and the solute molecule. This technique is interesting to enhance the statistics in the region near the solute, which is more relevant for the solute-solvent interaction and then more important to the subsequent quantum mechanics calculations.

A statistical analysis is needed to select configurations having small statistical correlation to carry out the QM calculations. Following the analysis of the autocorrelation functions of the energy and the calculation of the correlation interval,^{7,23} we selected configurations with less than 15% of statistical correlation to perform the QM calculations. At each iteration step of the polarization procedure, 100 configurations were used to calculate both the dipole moment (and the corresponding atomic charges) and the excitation energies in the UV-visible region. The INDO/CIS method, as implemented in the ZINDO program,³⁹ was employed to perform the excitation energy calculations.

C. Selection of solvation shells

The solvation shells are usually selected by analyzing the radial distribution function (RDF). Among several possibilities, it is the common procedure to use the RDF between the center of mass of the solute and solvent molecules. But this RDF is not appropriate when the solute has an elongated shape, as it was shown before.⁴⁰ For illustration in Fig. 2(a) we show a solvation shell of 45 water molecules selected using a center-of-mass RDF. One can see that the water molecules are not homogeneously distributed around the solute. Due to the shape of benzophenone, the water molecules at the left and right of the molecule are far from its center of mass and therefore only sparse water molecules near those edges are selected within the cutoff radius.

Therefore, to analyze the solvation shells of elongated molecules it is necessary to define a more convenient distri-

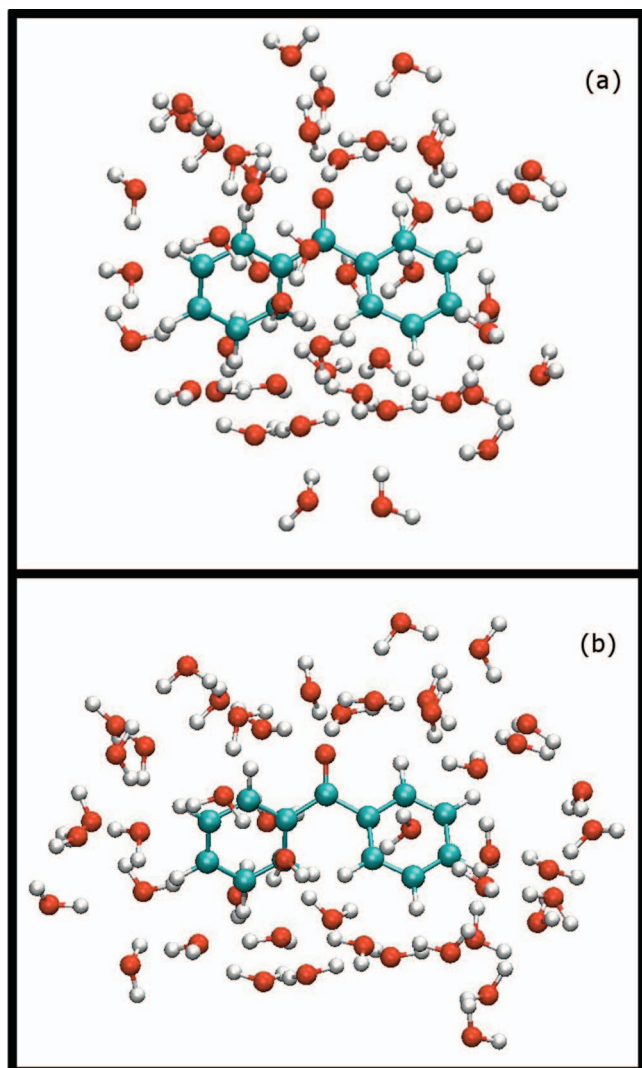


FIG. 2. (Color) A hydration shell of 45 molecules selected using the (a) center-of-mass RDF and (b) minimum-distance distribution function (MDDF).

bution function. A proper function to be used in this case seems to be a minimum-distance distribution function (MDDF) as suggested before for β -carotene⁴⁰ and further developed next for the general case. The MDDF is defined as

$$G(r) = \frac{\text{HISTOGRAM}[r_-, r_+]}{l\rho\delta V}, \quad (1)$$

where $r_+ = r + (\delta r/2)$, $r_- = r - (\delta r/2)$, l is the number of MC configurations used for computing the histogram, $\rho = N/V$ is the density of the system, and δr is the width of the bin of the histogram. The histogram is computed using only the smallest distance between all solute atoms and all solvent atoms. Hence, the shape of the molecule is automatically taken into account in the list of nearest neighbors. δV is the volume of a shell that corresponds to the type of normalization used. In a RDF, for instance, δV is the volume of the spherical shell whose radius comprises the range $[r_-, r_+]$ and is given by

$$\delta V = \frac{4\pi}{3}[(r_+)^3 - (r_-)^3]. \quad (2)$$

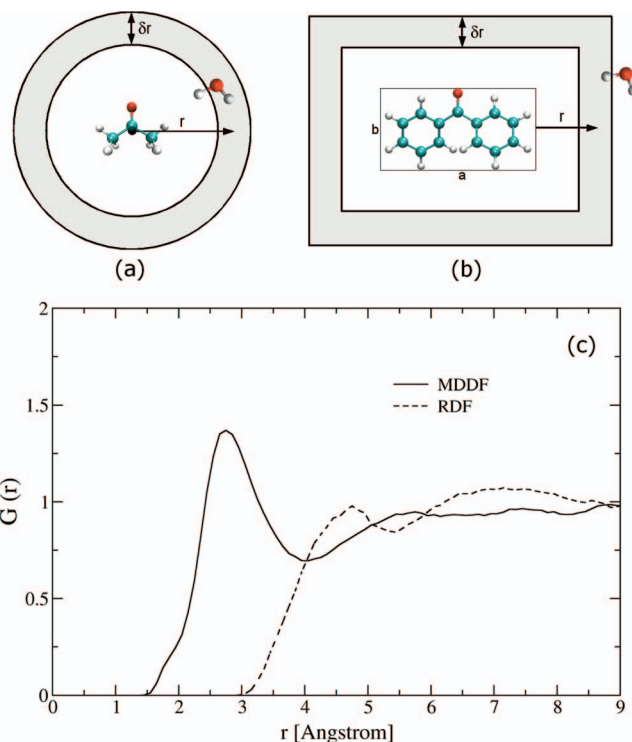


FIG. 3. (Color) Bidimensional illustration of the normalization shell volumes: (a) spherical shell used in the center-of-mass RDF and (b) parallelepiped shell used in the MDDF. Below (c) it is shown both distribution functions between benzophenone and water.

For the MDDF, however, there is no obvious choice for the form of the volume δV . In the present case we have chosen a parallelepiped normalization in which we fit the molecule to a box of dimensions a , b , and c . For benzophenone these dimensions are 11.5, 7.0, and 4.0 Å. The volume δV is then taken as the volume of the parallelepiped shell corresponding to a minimum distance in the range $[r_-, r_+]$ and is given by

$$\delta V = (a + 2r_+)(b + 2r_+)(c + 2r_+) - (a + 2r_-)(b + 2r_-)(c + 2r_-). \quad (3)$$

In Fig. 3 we illustrate the shell volume in a center-of-mass RDF [Fig. 3(a)] and in a MDDF with parallelepiped normalization [Fig. 3(b)]. Figure 3(c) shows the resulting MDDF and the conventional RDF involving the center of mass of the solute and the solvent. The MDDF shows a more structured first solvation shell compared to the RDF. In both cases it is hard to detect any structure of the solvent beyond the first shell.

In Fig. 2(b) we show a water shell with the same number of molecules (45) as before, now selected by the minimum-distance criterion instead of the center-of-mass distance. The solvent molecules are now more uniformly distributed around the benzophenone molecule compared to the RDF shell [Fig. 2(a)]. Of course, for small solutes, such as formaldehyde, the solvation shells selected with the MDDF and the center-of-mass RDF will be very similar.

Having considered all this, in each configuration, a ~ 9 Å thick solvation shell composed by the 235 nearest water molecules was selected through the MDDF to perform the

TABLE I. The five lowest excitation energies (cm^{-1}) of benzophenone in gas phase calculated with INDO/CIS.

Nature	Energy	Intensity	Experiment ^a
$n-\pi^*$	25 390	0.001	28 860 (weak)
$\pi-\pi^*$	36 157	0.007	
$\pi-\pi^*$	36 322	0.013	
$\pi-\pi^*$	39 796	0.255	40 400 (strong and broad)
$\pi-\pi^*$	40 662	0.047	

^aReferences 1 and 24.

quantum mechanics calculations. 100 configurations are sampled for the QM calculations in each case considered.

III. RESULTS AND DISCUSSION

A. Gas phase

In Table I we list the five lowest excitation energies of benzophenone in gas phase, corresponding to the bands found in the experimental UV-vis absorption spectrum. The $n-\pi^*$ transition energy is calculated at $25\,390\text{ cm}^{-1}$, below the experimental maximum^{1,24} in *n*-hexane at $28\,860\text{ cm}^{-1}$. There are also four calculated $\pi-\pi^*$ transitions. Two of them have weak intensity and are very close to each other at $\sim 36\,200\text{ cm}^{-1}$. They correspond to the shoulder observed at around $36\,000\text{ cm}^{-1}$ in the experimental spectrum in *n*-hexane. The more intense transition has a calculated energy of $39\,796\text{ cm}^{-1}$, but there is also a calculated $\pi-\pi^*$ transition of medium intensity nearby at $40\,662\text{ cm}^{-1}$. These two bands are the most intense and probably mix the intensities giving rise to the single broad and intense band seen in the experimental spectrum.^{1,24} The average of the two excitation energies, weighted by the intensities, gives an estimated theoretical maximum at $39\,930\text{ cm}^{-1}$, close to the experimental maximum observed in *n*-hexane at $40\,400\text{ cm}^{-1}$. In spite of a reasonably good description of the absorption spectrum of gas-phase benzophenone, our interest lies in the solvatochromic shift of these transitions and these have been well described by previous INDO/CIS studies.^{19,23,41–43}

B. Aqueous solution

1. Solute polarization

We now discuss the electronic polarization of the solute. The MP2/6-31++G(*d,p*) calculated dipole moment of isolated benzophenone is 3.11 D, very close to the gas-phase experimental value⁴⁴ of 2.98 D. Starting from this value, we

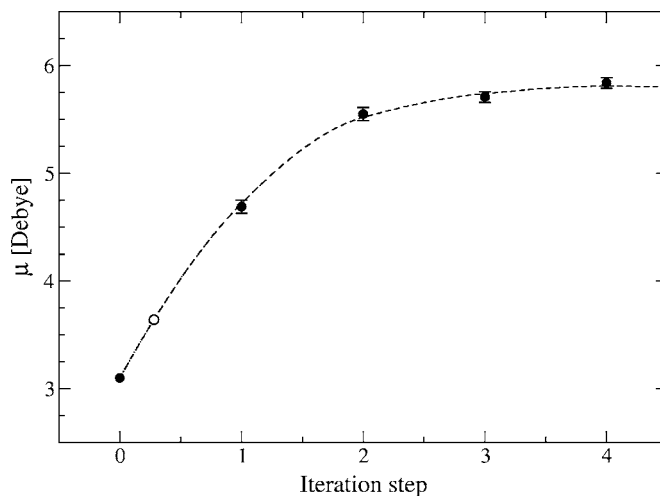


FIG. 4. Convergence of the dipole moment of benzophenone in water. The first step corresponds to the gas phase and the open circle represents the dipole given by the standard procedure to obtain the atomic charges (see text). The other points are averages over 100 configurations, with MP2/6-31++G(*d,p*).

iteratively applied the S-QM/MM method to obtain the dipole moment of the solute in water environment at room temperature and pressure. Figure 4 shows the behavior of the dipole moment during the iterative polarization procedure. Each point in the curve is the average of 100 calculations at the MP2/6-31++G(*d,p*) level except for the first value that is a single-point calculation of the gas-phase dipole moment.

As it can be seen, the dipole moment converges to the value of $5.84 \pm 0.05\text{ D}$ in the fourth step, as it is only 2% bigger than the dipole obtained in the third step. This seems to be typical and in the previous case of acetone¹⁹ the convergence was achieved with five iterations. Sánchez *et al.*, with the ASEP/MD approach, also reported that the convergence is usually achieved with 3–4 cycles.²⁹ The converged dipole moment of benzophenone in water is hence calculated as 88% larger than that of the gas phase. Such a great increase is understandable because the experimental polarizability of benzophenone is known and is relatively high⁴⁴ (around $144ea_0^3$) having two rings with polarizable π clouds. It is important to say that the isotropic polarizability of the molecule calculated in the same MP2/6-31++G(*d,p*) level is $153ea_0^3$ in good agreement with experiment. This means that the basis set is able to correctly reproduce the induced dipole moment of benzophenone. Table II shows the partial

TABLE II. Evaluation of the averaged atomic charges of the carbonyl group and dipole moments (μ in Debye) of the benzophenone in aqueous solution during the iteration procedure of its polarization. They are calculated with MP2/6-31++G(*d,p*) using 100 statistically uncorrelated MC configurations of the solution. The uncertainties are statistical errors (standard deviations are approximately ten times larger). For comparison the values obtained for the gas phase (iteration step 0) and for the standard procedure with HF/6-31G(*d*) are also shown.

Iteration step	0	1	2	3	4	Standard
$q(\text{O})$	-0.4570	-0.5712	-0.6340	-0.6568	-0.6636	-0.5464
$q(\text{C})$	0.4021	0.4701	0.5112	0.5186	0.5247	0.5113
μ	3.11	4.65 ± 0.066	5.55 ± 0.06	5.71 ± 0.05	5.84 ± 0.05	3.64

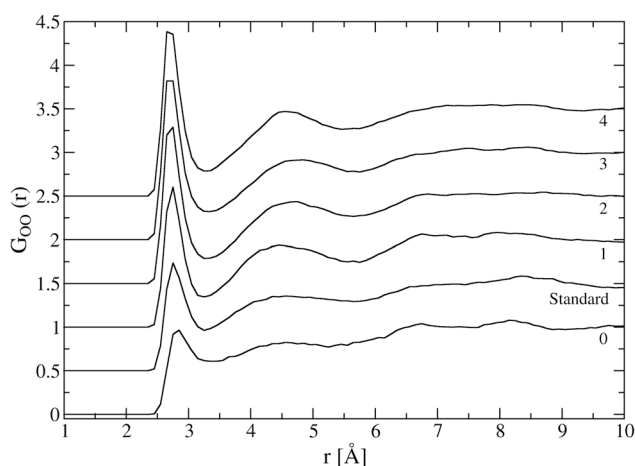


FIG. 5. RDFs between the oxygen of benzophenone and the oxygen of water. The functions are numbered according to the iteration step of the solute polarization procedure. For reference it is shown the RDF obtained with standard atomic charges (see text).

charges over the oxygen and the carbonyl carbon atoms, as well as the calculated dipole moments, along the polarization procedure.

For comparison, we simulated the water environment around benzophenone considering also the atomic charges obtained with the standard procedure of most common force fields,^{12,13} that is, the fitting of the electrostatic potential using CHELPG with a HF/6-31G(*d*) calculation. The dipole moment of 3.64 D was obtained with this procedure. In Fig. 4, this value is represented by an open circle and is an intermediate value between the gas-phase and the dipole obtained in the first iteration step of the polarization procedure. This dipole moment is only 17% larger than our theoretical gas-phase value and 22% larger than the experimental dipole⁴⁴ of 2.98 D. The appreciable difference between the dipole of the standard atomic charges and the converged in-solution dipole moment will have important effects on the solute-solvent interaction, as discussed below.

2. Solute-solvent interaction

First we discuss the influence of this in-solution polarization in the hydrogen bonds (HBs) between the solute and the solvent. In Fig. 5 we show the RDF between the oxygen atom of benzophenone and the oxygen atom of water. The first RDF (step 0), obtained using the gas-phase solute

charges, shows a little-structured first shell. With the polarization of the solute, this shell becomes more structured and its peak becomes sharper and is also shifted to a slightly smaller distance. Also, a second shell becomes discernible with a peak at around 4.5 Å.

Table III shows the number of HBs formed between benzophenone and water with the usual geometric-energetic criteria.^{45,46} In this case we used $R_{OO} \leq 3.5$ Å, $\theta_{OOH} \leq 40^\circ$, and $E_{\text{bind}} \geq 2.0$ kcal/mol. With gas-phase charges, there is an average of 1.27 HB between the solute and the solvent. With the standard atomic charges this number increases to 1.60 and with the polarized charges (step 4) it is further increased to 2.31 HBs. The strength of the HB also increases with the solute polarization, as it can be seen from Table IV. In the first step each HB has an average binding energy (E_{bind}) of 4.19 kcal/mol, whereas in the last step this energy is increased to 7.29 kcal/mol. These energies are calculated classically with the LJC potential.

Combining the increase of the number of HBs and the increase in the strength of each HB, one has a large increase of the binding energy due to this interaction from 5.3 kcal/mol with the gas-phase atomic charges (step 0) to 16.8 kcal/mol with the polarized charges (step 4). As expected, the total solute-solvent binding energy (E_{xs}) also increases from 29.8 kcal/mol in step 0 to 46.3 kcal/mol in step 4. In this regard, it is interesting to note that the difference in E_{xs} from step 3 to step 4 is only 0.8 kcal/mol, which is near $k_B T$. But the increase in E_{xs} does not follow that of the energy of the HBs. As it can be seen from R (sixth column in Table III), the fraction due to HB of the solute-solvent binding energy doubles from 18% to 36%. So, in this case, the HBs play a very important role in the polarization process.

Moreover, looking at the solute-solvent binding energy excluding the HB waters ($E_{\text{no-HB}}$ —last column in Table III), one can see that the binding energy of the solute with all the other molecules increases by only 5 kcal/mol (24.5 to 29.5 kcal/mol), whereas the binding energy due only to HBs increase 11.5 kcal/mol from step 0 to step 4. This indicates that the main response of the solvent structure to the polarization of the solute lies in the solute-solvent HB shell. This becomes even more evident if we separate the contribution of the solvent rearrangement in $E_{\text{no-HB}}$. This can be done if we use the permanent (gas phase) dipole moment of benzophenone on the configurations obtained in the polarization

TABLE III. The evolution of the energy associated with the solute-solvent hydrogen bonds during the iteration procedure of the solute polarization. The average number of HBs between benzophenone and water, the average binding energy per HB ($\langle E_{\text{bind}} \rangle / \text{HB}$), the total binding energy of HBs ($\langle E_{\text{bind}} \rangle$), and the total solute-solvent attractive energy ($\langle E_{\text{xs}} \rangle$) are given in kcal/mol. R is the ratio $\langle E_{\text{bind}} \rangle / \langle E_{\text{xs}} \rangle$, that is, the fraction of the energy due to the HBs, and $\langle E_{\text{no-HB}} \rangle$ is the difference $\langle E_{\text{xs}} \rangle - \langle E_{\text{bind}} \rangle$, that is, the solute-solvent energy not due to HBs.

Iteration	$\langle \text{HB} \rangle$	$\langle E_{\text{bind}} \rangle / \text{HB}$	$\langle E_{\text{bind}} \rangle$	$\langle E_{\text{xs}} \rangle$	R (%)	$\langle E_{\text{no-HB}} \rangle$
0	1.27	4.19	5.3	29.8	18	24.5
1	1.92	5.69	10.9	39.2	28	28.3
2	2.16	6.62	14.3	43.7	33	29.4
3	2.25	7.09	16.0	45.5	35	29.5
4	2.31	7.29	16.8	46.3	36	29.5
Standard	1.60	5.07	8.1	35.4	23	27.3

TABLE IV. The evolution of the solvatochromic shifts of the UV-vis spectrum (cm^{-1}) of benzophenone in aqueous solution during the iteration procedure of its polarization. The statistical errors associated with the calculated shifts are less than 40 cm^{-1} . The experimental shifts are 2200 and -1600 cm^{-1} , respectively, for the $n-\pi^*$ and the $\pi-\pi^*$ bands. See text.

Iteration Transition	0 Shift	1 Shift	2 Shift	3 Shift	4		Standard Shift
					Shift	Intensity	
$n-\pi^*$	988	1656	1875	1934	2045	0.003	1395
$\pi-\pi^*$	-203	-225	-243	-230	-244	0.021	-241
$\pi-\pi^*$	-384	-519	-541	-510	-569	0.027	-428
$\pi-\pi^*$	-1009	-1653	-1838	-1876	-1943	0.257	-1339
$\pi-\pi^*$	-695	-1098	-1256	-1242	-1363	0.064	-955

procedure. Hence, we subtract the induced charges of benzophenone in $E_{\text{no-HB}}$. Looking at the solute-solvent attractive energy (excluding the HBs) using the permanent (gas-phase) dipole moment of benzophenone at each step, the energy (not shown in Table III) increases only 1.3 kcal/mol from step 0 to step 4, showing that the rearrangement of the water molecules that are not making HB with the solute is negligible.

The reason for that is simple. The energy gained by the water molecules by interacting with the solute is small compared to the energy provided by the HB with other water molecules, and then the water molecules that do not make HB with benzophenone will not change appreciably their orientation because of the polarization. They sense, of course, the increase of the electrostatic field of the solute. But they do not respond significantly to that field with a sizable rearrangement.

3. Solvatochromic shifts

Now we turn to the solvatochromic shift of benzophenone in water. In Table IV we show the shifts for each step of the polarization procedure. The excitation energy in water is calculated considering a hydration shell composed of 235 molecules. All these molecules are considered explicitly in the INDO/CIS calculation. This means that the wave function, with 2148 valence electrons, is totally antisymmetric and is allowed to delocalize over the solvent, and therefore a contribution of the solvent polarization and dispersion interaction are included.⁴⁷ Each entry in Table IV is a statistically converged average over 100 configurations and the statistical errors (not shown to avoid congesting) are less than 40 cm^{-1} .

The $n-\pi^*$ shift obtained in the first step is $988 \pm 35 \text{ cm}^{-1}$. The intense $\pi-\pi^*$ transition is shifted by $-1009 \pm 30 \text{ cm}^{-1}$ and the fifth transition by $-695 \pm 25 \text{ cm}^{-1}$. By averaging these two last transitions, which are the most intense, weighted by the intensities, we have an estimate of $-920 \pm 25 \text{ cm}^{-1}$ for the shift of the $\pi-\pi^*$ band maximum. These shifts are improved when the standard atomic charges are used. The $n-\pi^*$ is shifted by $1395 \pm 35 \text{ cm}^{-1}$ and the $\pi-\pi^*$ by approximately $-1225 \pm 25 \text{ cm}^{-1}$ (again the average of the two last transitions). However, the experimental shifts^{1,24} are, respectively, 2200 and -1600 cm^{-1} . Hence, in the present case, although the standard procedure of obtaining the atomic charges represents a considerable improvement to

the solvatochromic shifts, it is not enough to lead to a quantitative description of the solvent effect on the absorption spectrum of the molecule.

The liquid structures generated with the equilibrated and polarized charges give a $n-\pi^*$ shift of $2045 \pm 40 \text{ cm}^{-1}$ and a shift on the $\pi-\pi^*$ maximum of $-1790 \pm 30 \text{ cm}^{-1}$. This represents a large difference of $\sim 650 \text{ cm}^{-1}$ to the blueshift obtained with standard procedure and $\sim 550 \text{ cm}^{-1}$ to the redshift. These values are now in good agreement with the experimental shifts, showing that the use of equilibrated and polarized charges is, in this case, necessary for an accurate description of the aqueous ambient around benzophenone and consequently a quantitative agreement of the solvatochromic shifts.

IV. SUMMARY AND CONCLUSIONS

The description of the absorption spectrum of benzophenone in water is a great theoretical challenge. Two diverse shifts are known in the experimental spectrum. A weak $n-\pi^*$ transition that is blueshifted and an intense and broad $\pi-\pi^*$ transition that is redshifted in water. Because of the large polarization of benzophenone in water a careful treatment of the in-solution electrostatic moments is necessary. In addition, the distribution of solvent molecules around the benzophenone requires special consideration because of its elongated shape. This has been addressed by considering not the usual spherical distribution given by RDFs, but instead, by a MDDF. To account for the solute polarization, an iterative procedure, based on the sequential QM/MM methodology, was applied to obtain the dipole moment of benzophenone in water at normal conditions. At each step, the dipole moment of the solute and the corresponding atomic charges are calculated with MP2/6-31++G(d,p) in the presence of water for several statistically uncorrelated configurations. The calculated charges are averaged and used to generate a new solvent structure, which further polarizes the solute. This is carried on until the convergence in the dipole moment is achieved and the electronic distribution is in electrostatic equilibrium with the solvent. The calculated average dipole moment of benzophenone in water converges to the value of $5.84 \pm 0.05 \text{ D}$. This is 88% larger than the gas-phase value of 3.11 D . This value can also be compared with the case of acetone,¹⁹ a less polarizable system, where the in-water polarization leads to an increase of 60%, in good agreement

with the value obtained from *ab initio* Car-Parrinello molecular dynamics.⁴⁸ To probe the in-solution dipole moment of benzophenone and the corresponding solute polarization, we used the converged atomic charges in the electrostatic potential of an extra simulation. Using uncorrelated configurations, and solvation shells defined by a minimum-distance distribution, we calculated the excitation energies with INDO/CIS method and obtained the $n-\pi^*$ shift of $2045 \pm 40 \text{ cm}^{-1}$ and an estimated $\pi-\pi^*$ shift (weighted by the intensity of two transitions) of $-1790 \pm 30 \text{ cm}^{-1}$. These results are in good agreement with the experimental values of 2200 and -1600 cm^{-1} , respectively. Using the standard procedure to generate the atomic charges (corresponding to a dipole moment of 3.64 D), the average shifts are calculated as 1395 ± 35 and $-1225 \pm 25 \text{ cm}^{-1}$, both about 600 cm^{-1} smaller in magnitude than the converged values.

This study gives the first full description of the entire UV-vis absorption spectrum of benzophenone in water. The results corroborate that, in many cases, a careful consideration of the solute polarization is essential to describe the solute-solvent interaction and the electronic properties of polar molecules in polar environment. Also, the conventional description of solvent shells might be revised for molecular solutes with a general shape. This can be done using the minimum-distance distribution function considered here.

ACKNOWLEDGMENTS

The authors thank Rafael C. Barreto for helpful discussions. This work has been partially supported by the Brazilian agencies FAPESP, CNPq, and CAPES.

- ¹C. Reichardt, *Solvent and Solvent Effects in Organic Chemistry*, 3rd ed. (Wiley-VCH, Weinheim, 2003).
- ²L. Onsager, *J. Am. Chem. Soc.* **58**, 1486 (1936).
- ³J. G. Kirkwood, *J. Chem. Phys.* **2**, 351 (1934).
- ⁴For reviews, see J. Tomasi, *Theor. Chem. Acc.* **112**, 184 (2004); J. Tomasi, B. Mennucci, and R. Cammi, *Chem. Rev. (Washington, D.C.)* **105**, 2999 (2005).
- ⁵J. T. Blair, K. Krogh-Jespersen, and R. M. Levy, *J. Am. Chem. Soc.* **111**, 6948 (1989); A. Warshel and M. Levitt, *J. Mol. Biol.* **103**, 227 (1976).
- ⁶K. Coutinho and S. Canuto, *Adv. Quantum Chem.* **28**, 89 (1997).
- ⁷K. Coutinho and S. Canuto, *J. Chem. Phys.* **113**, 9132 (2000); K. Coutinho, S. Canuto, and M. C. Zerner, *ibid.* **112**, 9874 (2000).
- ⁸K. Aidas, J. Kongsted, A. Osted, K. V. Mikkelsen, and O. Christiansen, *J. Phys. Chem. A* **109**, 8001 (2005); J. Kongsted, A. Osted, K. V. Mikkelsen, and O. Christiansen, *J. Chem. Phys.* **118**, 1620 (2003); T. D. Poulsen, P. R. Ogilby, and K. V. Mikkelsen, *ibid.* **115**, 7843 (2001); L. Jensen, P. Th. van Duijn, and J. G. Snijders, *ibid.* **119**, 3800 (2003).
- ⁹K. Naka, A. Morita, and S. Kato, *J. Chem. Phys.* **111**, 481 (1999).
- ¹⁰C. J. R. Illingworth, S. R. Gooding, P. J. Winn, G. A. Jones, G. G. Ferenczy, and C. A. Reynolds, *J. Phys. Chem. A* **110**, 6487 (2006).
- ¹¹J. Gao and X. Xia, *Science* **258**, 631 (1992).
- ¹²J. Pranata, S. G. Wierschke, and W. L. Jorgensen, *J. Am. Chem. Soc.* **113**, 2810 (1991); W. D. Cornell, P. Cieplak, C. I. Bayly, I. R. Gould, K. M. Merz, Jr., D. M. Ferguson, D. C. Spellmeyer, T. Fox, J. W. Caldwell, and P. A. Kollman, *J. Am. Chem. Soc.* **117**, 5179 (1995).

- ¹³N. A. McDonald, H. A. Carlson, and W. L. Jorgensen, *J. Phys. Org. Chem.* **10**, 563 (1997).
- ¹⁴M. E. Martin, M. L. Sánchez, F. J. Olivares del Valle, and M. A. Aguilar, *J. Chem. Phys.* **113**, 6308 (2000); M. L. Sánchez, M. E. Martín, M. A. Aguilar, and F. J. Olivares del Valle, *J. Comput. Chem.* **21**, 705 (2000).
- ¹⁵S. Chalmet and M. F. Ruiz-López, *J. Chem. Phys.* **115**, 5220 (2001).
- ¹⁶P. L. Silvestrelli and M. Parrinello, *Phys. Rev. Lett.* **82**, 3308 (1999).
- ¹⁷K. Coutinho, R. C. Guedes, B. J. Costa Cabral, and S. Canuto, *Chem. Phys. Lett.* **369**, 345 (2003); R. Rivelino, B. J. Costa Cabral, K. Coutinho, and S. Canuto, *ibid.* **407**, 13 (2005).
- ¹⁸T. Ohba and S. Ikawa, *Mol. Phys.* **73**, 985 (1991).
- ¹⁹H. C. Georg, K. Coutinho, and S. Canuto, *Chem. Phys. Lett.* **429**, 119 (2006).
- ²⁰W. P. Hayes and C. J. Timmons, *Spectrochim. Acta* **21**, 529 (1965).
- ²¹N. S. Bayliss and E. G. McRae, *J. Phys. Chem.* **58**, 1006 (1954).
- ²²N. S. Bayliss and G. Wills-Johnson, *Spectrochim. Acta, Part A* **24**, 551 (1968).
- ²³K. Coutinho and S. Canuto, *J. Mol. Struct.: THEOCHEM* **632**, 235 (2003).
- ²⁴W. L. Dilling, *J. Org. Chem.* **31**, 1045 (1966).
- ²⁵G. E. Bennett and K. Johnston, *J. Phys. Chem.* **98**, 441 (1994).
- ²⁶S. Urahata and S. Canuto, *Int. J. Quantum Chem.* **80**, 1062 (2000).
- ²⁷J. Ridley and M. C. Zerner, *Theor. Chim. Acta* **32**, 111 (1973).
- ²⁸C. M. Breneman and K. B. Wiberg, *J. Comput. Chem.* **11**, 361 (1990).
- ²⁹M. L. Sánchez, M. E. Martín, M. A. Aguilar, and F. J. Olivares del Valle, *Chem. Phys. Lett.* **310**, 195 (1999); M. E. Martín, M. L. Sánchez, F. J. Olivares del Valle, and M. A. Aguilar, *J. Chem. Phys.* **113**, 6308 (2000).
- ³⁰P. L. Muñio and P. R. Callis, *J. Chem. Phys.* **100**, 4093 (1994).
- ³¹K. Ando, *J. Chem. Phys.* **107**, 4585 (1997); F. Cichos, R. Brown, and Ph. A. Bopp, *ibid.* **114**, 6834 (2001).
- ³²M. P. Allen and D. J. Tildesley, *Computer Simulation of Liquids* (Clarendon, Oxford, 1987).
- ³³K. Coutinho and S. Canuto, DICE, a Monte Carlo program for molecular liquid simulation, University of São Paulo, São Paulo, Brazil, 2003.
- ³⁴H. J. C. Berendsen, J. P. M. Postma, W. F. van Gunsteren, and J. Hermans, in *Intermolecular Forces*, edited by B. Pullman (Reidel, Dordrecht, 1981), p. 331.
- ³⁵E. B. Fleischer, N. Sung, and S. Hawkinson, *J. Chem. Phys.* **72**, 4311 (1968).
- ³⁶M. J. Frisch, G. W. Trucks, H. B. Schlegel *et al.*, Gaussian 98, Revision A.11.4, Gaussian Inc., Pittsburgh, PA, 2002.
- ³⁷W. L. Jorgensen, D. S. Maxwell, and J. Tirado-Rives, *J. Am. Chem. Soc.* **118**, 11225 (1996).
- ³⁸J. C. Owlicki and H. A. Scheraga, *Chem. Phys. Lett.* **47**, 600 (1977).
- ³⁹M. C. Zerner, ZINDO, a semi-empirical program package, University of Florida, Gainesville, FL, 1996.
- ⁴⁰S. Canuto, K. Coutinho, and D. Trzesniak, *Adv. Quantum Chem.* **41**, 161 (2002).
- ⁴¹M. Z. Hernandez, R. Longo, K. Coutinho, and S. Canuto, *Phys. Chem. Chem. Phys.* **6**, 2088 (2004).
- ⁴²R. Rivelino, K. Coutinho, and S. Canuto, *J. Phys. Chem. B* **106**, 12317 (2002).
- ⁴³W. R. Rocha, K. J. de Almeida, K. Coutinho, and S. Canuto, *Chem. Phys. Lett.* **345**, 171 (2001).
- ⁴⁴J. W. Barker and L. J. Noe, *J. Chem. Phys.* **57**, 3035 (1972).
- ⁴⁵S. Canuto and K. Coutinho, *Int. J. Quantum Chem.* **77**, 192 (2000); T. Malaspina, K. Coutinho, and S. Canuto, *J. Chem. Phys.* **117**, 1692 (2002).
- ⁴⁶W. L. Jorgensen, J. Chandrasekar, J. D. Madura, R. W. Impey, and M. L. Klein, *J. Chem. Phys.* **79**, 926 (1983).
- ⁴⁷S. Canuto, K. Coutinho, and M. C. Zerner, *J. Chem. Phys.* **112**, 7293 (2000).
- ⁴⁸U. F. Röhrig, I. Frank, J. Hutter, A. Laio, J. Vandevondele, and U. Rothlisberger, *ChemPhysChem* **4**, 1177 (2003).